Compositional Grid Codes with Guarantee on Both Stability and Dynamic Performance

Xiaoyu Peng, Cong Fu, Zhongze Li, Xi Ru, Zhaojian Wang, Feng Liu, *Senior Member, IEEE*

***Abstract*— This paper proposes a compositional grid code framework that guarantees power system stability and dynamic performance simultaneously. By reformulating device-grid interactions based on passivity theory, we derive compositional stability indices compatible with heterogeneous dynamics. Then, the proposed grid codes decompose system-level stability certificates into quantitative constraints upon individual devices while accommodating standard dynamic specifications. Compared with existing approaches, this method overcomes the previous limitations in closed-loop stability assurance and facilitates the plug-and-play integration of heterogeneous dynamic devices.**

***Index Terms*—Grid code, distributed stability criteria, and passivity.**

I. Introduction

Power systems maintain safe and stable operations by guaranteeing the *grid codes*, a set of standardized technical requirements. Traditional centralized frameworks for satisfying these codes are challenged by the integration of massive inverter-based resources (IBRs). To address this issue, the compositional implementation of grid codes has been proposed. Under this paradigm, system operators (SOs) define *mandatory* grid codes based on real-time operation conditions and disseminate them to individual devices. Each device then locally adjusts its control to comply with these codes, enabling compositional coordination of system-level dynamics. Crucially, the model-independent nature of this paradigm enables its applications to black/gray-box devices. The IBRs' grid codes are initially designed for grid-following (GFL) devices [1] and then extended to grid-forming (GFM) ones [2], [3].

Grid codes should encompass two critical aspects: stability and dynamic performance specifications. The latter is quantified by the critical indices of time-domain responses under specific disturbances [1], [2]. While existing research primarily focuses on it, stability remains overlooked even in a small-signal sense. The transfer-function design is investigated in [1] to meet the grid codes for fast frequency responses. Then, it is extended to AC/DC hybrid systems with standardizable grid code disaggregation methods [4]. However, they cannot guarantee closed-loop stability of the systems and thus might not be applicable in grids with weak stability support.

Incorporating stability into grid code design necessitates decomposing system-level stability certificates into device-level indices. Passivity theory offers a viable foundation due to its scalability and state-independence, since the feedback or parallel connection of passive subsystems is still passive as a closed-loop system, which further implies the stability [5]. However, the non-passive nature of typical devices (e.g., virtual synchronous generator, VSGs) in high-frequency bands serves as a common issue for passivity-based methods even in electromechanical models [6]. To overcome this problem, the literature employs a switching formulation, i.e., using polar coordinates in low-frequency bands and turning to rectangular coordinates in high-frequency bands [7]. However, despite its efficiency in stability assessment, the method exhibits limited applicability to grid code generation since the latter are usually predetermined through metrics of polar quantities.

By reformulating the topological structure and output mapping of the passivity definition, we derive a novel passivity-based index to address the above two problems. On this basis, we present a unified and scalable framework for grid code synthesis, integrating both stability and dynamic performance considerations. In contrast to existing literature, it fills the gap in the stability assurance of grid codes with extended compatibility to heterogeneous devices.

Notation: For a symmetrical matrix M, let $\lambda_{\min}(M)$ denote its minimum eigenvalue and $M \succ 0$ for its positive definiteness. $M^{\dagger}$ stands for the Moore–Penrose pseudo-inverse.

II. Formulation of Power System Dynamics

Consider an n-bus power system $\mathscr{G} = \mathscr{G}(\mathscr{V}, \mathscr{E})$, where $\mathscr{V}$ and $\mathscr{E}$ are the set of buses and transmission lines, respectively. Each bus $i \in \mathscr{V}$ has port-wise dynamics $(V_i, \theta_i, P_i, Q_i)$ representing voltage magnitude, phase-angle, active and reactive power in order. The vector form $V = [V_1, V_2, \cdots, V_n]^T$ is employed and similar for θ, P and Q.

1) Network Model: The transmission network dynamics is described by the power flow equation $P_i + jQ_i = V_i \sum_{j\in\mathscr{V}} V_j B_{ij}(\sin\theta_{ij} - j\cos\theta_{ij})$, $\forall i \in \mathscr{V}$. Linearizing it around an equilibrium $[V^*, \theta^*]^T$ yields:

$$\begin{bmatrix}\Delta P \\ \Delta \frac{Q}{V}\end{bmatrix} = \begin{bmatrix}A & D \\ D^T & C\end{bmatrix}\begin{bmatrix}\Delta\theta \\ \Delta V\end{bmatrix} \stackrel{\text{def}}{=} H \begin{bmatrix}\Delta\theta \\ \Delta V\end{bmatrix} \tag{1}$$

where $A = \partial P/\partial\theta$, $C = \partial(Q/V)/\partial V$ and $D = \partial P/\partial V = [\partial(Q/V)/\partial\theta]^T$. Their entry-wise expressions can be found in [8]. Δ denotes the increment w.r.t. the steady values.

This paper is supported by the Science and Technology Project of China Southern Power Grid Co., Ltd under Grant 036000KC23090004 (GDKJXM20231026). (*Corresponding Author: Feng Liu*).

Xiaoyu Peng, Zhongze Li, Xu Ru, and Feng Liu are with Department of Electrical Engineering, Tsinghua University, Beijing, China (email: pengxy19@tsinghua.org.cn, lizz24@mails.tsinghua.edu.cn, thu.ruxi@gmail.com, lfeng@tsinghua.edu.cn).

Cong Fu is with Guangdong Power Grid Co., Ltd, Guangzhou, China (email: 609511305@qq.com).

Zhaojian Wang is with Department of Automation, Shanghai Jiao Tong University, Shanghai, China (email: wangzhaojian@sjtu.edu.cn).

2) Device Dynamics: The dynamics of inverters vary depending on their control strategies. For compatibility, here we adopt a unified model (2) for device $i \in \mathscr{V}$.

$$-\begin{bmatrix}\Delta\theta_i\\ \Delta V_i\end{bmatrix} = \begin{bmatrix}G_{\theta,i}(s) & \\ & G_{V,i}(s)\end{bmatrix}\begin{bmatrix}\Delta P_i\\ \Delta\frac{Q_i}{V_i}\end{bmatrix} \stackrel{\text{def}}{=} G_i(s)\begin{bmatrix}\Delta P_i\\ \Delta\frac{Q_i}{V_i}\end{bmatrix} \tag{2}$$

Specific forms of G_i for common devices are introduced in Section IV, and more details can be found in [9].

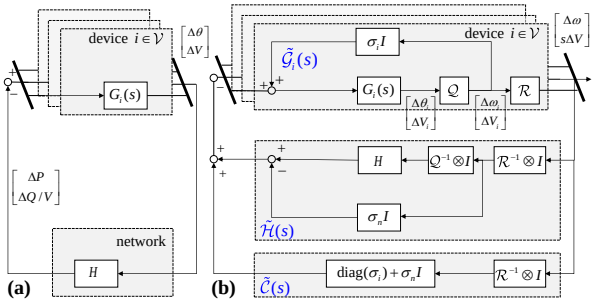

Fig. 1. Feedback interconnected power system model. (a): original model. (b): equivalent passive model, where $\mathcal{Q} = \text{diag}(s, 1)$ and $\mathcal{R} = \text{diag}(1, s)$.

Combining the network (1) and device models (2), the system can be formulated into a feedback-interconnected form of $\mathscr{G}$ depicted in Fig.1(a). Then, this paper focuses on the small-signal stability of the closed-loop system $\mathscr{G}$.

III. Passivity-based Distributed Stability Criteria

Definition 1 (*Passivity* [5])**.** A system $\dot{x} = f(x, u)$, $y = h(x, u)$ is passive if there exists a continuously differentiable $S(x) \geq 0$ s.t. $u^T y \geq \dot{S} = \partial S/\partial x \cdot f(x, u)$, $\forall (x, u)$.

Passivity of linear systems can be verified by frequency-domain transfer functions, as detailed in the following lemma, a straightforward corollary of [5] considering the relation between passivity and positive real.

Lemma 1. Consider a linear time-invariant system with minimal realization $\dot{x} = Ax + Bu, y = Cx + Du$. It is passive if its transfer function $T(s) = C(sI - A)^{-1}B + D$ satisfies

(a). Poles of all elements of $T(s)$ are in the closed-left-half plane.
(b). For all real ω for which $j\omega$ is not a pole of any element of $T(s)$, the matrix $T(j\omega) + T^T(-j\omega) \succeq 0$.
(c). Any pure imaginary pole $j\omega$ of any element of $T(s)$ is a simple pole and the residue $\lim_{s\to j\omega}(s - j\omega)T(s) \succeq 0$.

Due to the non-passive nature of the original system in Fig.1(a), we first transform it into Fig.1(b), where the linear operators are $\mathcal{Q} = \text{diag}(s, 1), \mathcal{R} = \text{diag}(1, s)$. The original network model usually has a negative minimal eigenvalue $\lambda_{\min}(H) < 0$ named network reversal in [8] and thus $H + H^T = 2H \not\succeq 0$. Therefore, it is not passive since it does not satisfy the condition (b) of Lemma 1. For the passivity-based stability assessment, it is essential to transform it into Fig.1(b), which introduces the output-feedback and input-feedforward passivity indices. This transformation enables the passivity of both networks and devices, as discussed later in Section IV. Mathematically, it is straightforward to verify the equivalence between Fig.1(a) and (b) by the block diagram transformation technique. Physically, the impact of $\mathcal{Q} \cdot G_i$ is to set the devices' interfaces with input $[\Delta P, \Delta(Q/V)]^T$ and output $-[\Delta\omega, \Delta V]^T$ (distinct from original $-[\Delta\theta, \Delta V]^T$), where $\Delta\omega = s\Delta\theta$ is the frequency deviation. Now we are ready to present the main theory of this letter.

Theorem 1. A power system $\mathscr{G}$ is small-signal stable if all the following conditions are satisfied:

(a). **Equilibrium condition**: the steady-state phase-angle deviation $|\theta_{ij}^*| = |\theta_i^* - \theta_j^*| < \pi/2, \forall (i, j) \in \mathscr{E}$.
(b). **Device condition**: there exist a $\sigma_i > 0$ s.t. $\tilde{\mathcal{G}}_i$ is passive, $\forall i \in \mathscr{V}$, where

$$\tilde{\mathcal{G}}_i(s) := \mathcal{R}(I - \sigma_i \mathcal{Q} G_i)^{-1}\mathcal{Q}G_i \tag{3}$$

(c). **Network condition**: each device $i \in \mathscr{V}$ satisfies $\sigma_i + \sigma_n > 0$, where $\sigma_n = \min[\lambda_{\min}(C - D^T A^\dagger D), 0]$.

Proof. We first prove the passivity of three subsystems, $\tilde{\mathcal{G}}$, $\tilde{\mathcal{C}}$ and $\tilde{\mathcal{H}}$ in Fig.1(b). The first two are directly guaranteed by conditions (b) and (c). Hence, we only need to check $\tilde{\mathcal{H}}$.

$\tilde{\mathcal{H}}$ satisfies the conditions of Lemma 1 as proved below: condition (a) is naturally satisfied and (b) $\tilde{\mathcal{H}}(j\omega) + \tilde{\mathcal{H}}^T(-j\omega) = \text{diag}(-\sigma_n I, 0) \geq 0$ holds if and only if $\sigma_n \leq 0$. Condition (c) is $\lim_{s\to 0} s\tilde{\mathcal{H}}(s) = [A, D; D^T, C - \sigma_n I] \succeq 0$. According to the generalized Schur's theorem [8], the above matrix is positively definite if and only if $A \succeq 0$ and $C - \sigma_n I - D^T A^\dagger D \succeq 0$. While $A \succeq 0$ has been guaranteed by condition (a) of this theorem, the latter can be achieved by letting $\sigma_n < \lambda_{\min}(C - D^T A^\dagger D)$. Therefore, $\tilde{\mathcal{H}}$ is passive if $\sigma_n \leq \min[\lambda_{\min}(C - D^T A^\dagger D), 0]$.

The feedback interconnected system is still passive if all subsystems are passive [5, Theorem 6.3]. Therefore, the closed-loop system is passive and further stable [5, Theorem 6.4], which completes the proof. □

IV. Compositional Grid Codes

This letter considers the grid code w.r.t. the device dynamics (4), which aligns with the widely employed VSG dynamics. It focuses on the electromechanical dynamics such as synchronization and voltage control loops, typically below $10^0 - 10^1$ Hz in the dq reference frame, which serve as the common form for grid code design and primary concerns of transmission SOs [4]. The analysis does not cover higher-frequency electromagnetic transients, as these are usually local and not a priority for grid code compliance.

$$G_{\theta,i} = 1/[s(M_i s + d_i)],\ G_{V,i} = 1/(\tau_i s + k_i) \tag{4}$$

where M_i, d_i, τ_i, k_i correspond to frequency inertia and damping, voltage time constant and damping. Systematic methods to generate device frequency-domain grid codes can be found in [1]. Due to the high compatibility of the proposed method, it is also applicable to other dynamic forms apart from VSG-like ones if required, such as $P - f/Q - V$ droop and time-domain response dynamics as demonstrated in Appendix A.

[1] Next, we derive twofold grid codes: stability and dynamic performance of systems.

A. Grid Code for Stability Guarantee

Substituting (4) into (3) yields $\tilde{\mathcal{G}}_i(s) = \mathrm{diag}(1/(M_i s + d_i - \sigma_i), s/(\tau_i s + k_i - \sigma_i)$. To ensure $\tilde{\mathcal{G}}_i$ passive, it is necessary solely for $d_i - \sigma_i > 0$ and $k_i - \sigma_i > 0$ to meet condition (a) of Lemma 1. The condition (b) can be guaranteed by the relative order 1 of $\tilde{\mathcal{G}}_i$, and (c) is trivial. Therefore, the stability grid code of (2) w.r.t. a desired σ_i^{des} is:

$$\boxed{d_i \geq \sigma_i^{\mathrm{des}}, k_i \geq \sigma_i^{\mathrm{des}}} \tag{5}$$

By setting $\sigma_i^{\mathrm{des}} > -\sigma_n$ for each device $i \in \mathscr{V}$, the stability can be guaranteed according to Theorem 1.

Relation with DP index [6]: The proposed index σ_i is an extension of the DP index. The latter shares the same framework in Fig.1(b) but with $\mathcal{Q}' = \mathrm{diag}(1,1)$ and $\mathcal{R}' = \mathrm{diag}(s,s)$. The network can retain the same index $\sigma_n' = \sigma_n = \lambda_{\min}(C - D^T A^\dagger D) < 0$ for the original DP theory under the conditions of Theorem 1. [2] Therefore, either $\sigma_i > -\sigma_n$ or $\sigma_i' > -\sigma_n$ can guarantee the stability, which extends the applicability of the DP index.

Corollary 1. *$\mathscr{G}$ is stable if the conditions of Theorem 1 are satisfied with either $\mathcal{Q}, \mathcal{R}$ or $\mathcal{Q}', \mathcal{R}'$ for each device.*

On the device side, the proposed index is compatible with those suitable for the DP index, as shown in Appendix A. Moreover, it addresses dynamics that the original DP theory cannot handle. Focusing on the VSG dynamics (4), $\tilde{\mathcal{G}}_i'(s) = \mathrm{diag}[1/[s(M_i s + d_i) - \sigma_i'], 1/(\tau_i s + k_i - \sigma_i')]$ cannot be passive for any given $\sigma_i' \geq 0$ in the original DP theory. Therefore, the DP index cannot identify the stability and is thus not applicable for grid code synthesis. Readers interested in a deeper exploration may refer to Appendix B.

B. Grid Code for Dynamic Performance Guarantee

The dynamic performance codes are typically prescribed in terms of time-domain characteristics, but they can be transformed into frequency-domain indices using standard methods [1]. Still take the dynamic form (4) as an example. Then, the dynamic code *maximum rate-of-change-of-frequency (ROCOF)* $\max|\dot{\omega}|_i^{\mathrm{des}} \leq \alpha_i$ *under normalized power disturbance* equals to $M_i^{\mathrm{des}} \geq 1/\alpha_i$. Similarly, the code *maximum steady frequency deviation* $\max|\Delta\omega_\infty|_i^{\mathrm{des}} \leq \beta_i$ equals $d_i^{\mathrm{des}} \geq 1/\beta_i$. Likewise, the time-domain grid code can be equivalently transformed into parameter requirements.

$$\boxed{M_i \geq M_i^{\mathrm{des}},\ d_i \geq d_i^{\mathrm{des}},\ \tau_i^{\mathrm{des}} \geq \tau_i,\ k_i \geq k_i^{\mathrm{des}}} \tag{6}$$

[1] Because of the space limitation, all appendices in this article are omitted, which can be found in https://github.com/lingo01/Compositional_Grid_Code.

[2] The index σ_n quantifies the network's desynchronization impact. $\lambda_{\min}(C - D^T A^\dagger D) < 0$ generally holds for power grids [6], [8].

C. Composition Property

In power systems, certain devices might lack or have very weak regulation capabilities and thus hardly meet grid codes by themselves. This part demonstrates that their deficiencies can be compensated by the support of other devices, enabling the cluster to satisfy the grid code, and the basic idea is inspired by the pioneering works [4]. Specifically, consider a bus $i \in \mathcal{V}$ connected to a cluster of devices interconnected via a radial network, denoted as $\mathcal{V}_{i_l} = \{i_l\}_{l=1}^m = \{i_1, i_2, \ldots, i_m\} \subset \mathcal{V}$. The topology widely exists for renewable energy stations.

Still take G_θ as an example. As the devices connected to $i \in \mathcal{V}_{i_l}$ are electrically close to each other, it is reasonable to assume that their dynamics are similar and the power losses on these lines $(i_l, i) \in \mathscr{E}$ are negligible [4], i.e., $\Delta\theta_{i_l} \approx \Delta\theta_i$, $\sum_l \Delta P_{i_l} \approx \Delta P_i$. Since each device satisfies $\Delta\theta_{i_l} = -G_{\theta,i_l}(s)\Delta P_{i_l}$, summing over all $\{i_1, i_2, \ldots, i_m\}$ yields $\sum_l -G_{\theta,i_l}^{-1}(s)\Delta\theta_{i_l} \approx \sum_l -G_{\theta,i_l}^{-1}(s)\Delta\theta_i = \sum_l \Delta P_{i_l} \approx \Delta P_i$. Combining it with $\Delta\theta_i = -G_{\theta,i}(s)\Delta P_i$, we obtain:

$$\sum_{l\in\mathcal{V}_{i_l}} G_{\theta,i_l}^{-1}(s) = G_{\theta,i}^{-1}(s) \tag{7}$$

Similarly, the voltage dynamics can be aggregated by $\sum_l G_{V,i_l}^{-1}(s) = G_{V,i}^{-1}(s)$.

1) Parameter Composition Property: We first investigate the parameter composition assuming all devices still take the form of (4). Then (7) yields $G_{\theta,i}(s) = 1/[s((\sum_l M_{i_l})s + \sum_l d_{i_l})]$. In other words, the whole station is equivalent to a device with inertia $\sum_l M_{i_l}$ and damping $\sum_l d_{i_l}$. Similarly, for voltage dynamics, the station can be considered as having an equivalent voltage time constant $\sum_l \tau_{i_l}$ and voltage damping $\sum_l k_{i_l}$. Therefore, the aggregated dynamics at the i-th bus:

- The stability code only requires $\min(\sum_l d_{i_l}, \sum_l k_{i_l}) \geq \sigma_i^{\mathrm{des}}$, rather than requiring every individual device $i_l \in \mathcal{V}$ to satisfy $\min(d_{i_l}, k_{i_l}) \geq \sigma_{i_l}^{\mathrm{des}}$.
- The dynamic code only requires $\sum_l M_{i_l} \geq M_i^{\mathrm{des}}$ and $\sum_l \tau_{i_l} \geq \tau_i^{\mathrm{des}}$, rather than requiring every individual device $i_l \in \mathcal{V}$ to satisfy $M_{i_l} \geq M_{i_l}^{\mathrm{des}}$ and $\tau_{i_l} \geq \tau_{i_l}^{\mathrm{des}}$.

2) Dynamic Form Composition Property: Several devices in the cluster might not be controllable to satisfy the dynamics (4). Suppose the devices $\mathcal{V}_{i_l}$ can be divided into controllable set $\mathcal{V}_{i_l}^{\mathcal{C}}$ and non-controllable one $\mathcal{V}_{i_l}^{\mathcal{N}}$. Then, the desired dynamics $G_{\theta,i}^{-1}(s) =$(4) can still be achieved by letting $\sum_{i\in\mathcal{V}_{i_l}^{\mathcal{C}}} G_{\theta,i_l}^{-1}(s) = G_{\theta,i}^{-1}(s) - \sum_{i\in\mathcal{V}_{i_l}^{\mathcal{N}}} G_{\theta,i_l}^{-1}(s)$. Specifically, we refer to [1] for how to allocate control gains of different controllable devices. Moreover, by employing the causal inverse method in [4], the proposed framework can also consider the GFL dynamics, and the composition property still holds.

Therefore, through the above composition property, the applicability of the proposed grid code is significantly extended.

D. Device-Network Interaction through Grid Codes

Fig.2 shows the online rolling update for device-network interaction using grid codes, ensuring stability and dynamic performance, partly accounting for the nonlinear and time-varying nature of power systems.

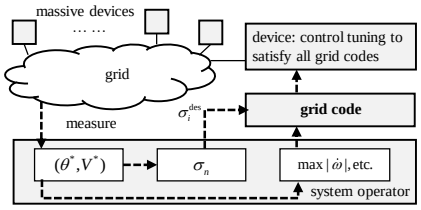

Fig. 2. Procedure of device-network interaction through grid codes.

(a). **SOs** *measure and estimate* the equilibrium (V^*, θ^*) and compute the real-time index σ_n (or use a static and conservative value derived from historical statistics).

(b). **SOs** *decide and distribute* the grid codes, including two parts: 1) stability code $\sigma_i^{\text{des}} = -\sigma_n + \Delta\sigma_{\text{margin}}$, where $\Delta\sigma_{\text{margin}}$ quantifies the stability margin. 2) dynamic performance code such as $\max|\dot{\omega}|_i^{\text{des}}$ and $\max|\Delta\omega_\infty|_i^{\text{des}}$.

(c). **Device clusters** *adjust* the controls and parameters to satisfy the grid code. For example, a device with dynamics (4) should satisfy (5) and (6).

V. Case Study

The proposed method is verified on an IEEE 118-bus system with the basic settings provided in [9]. The dynamics code is $(M_i^{\text{des}}, d_i^{\text{des}}, \tau_i^{\text{des}}, k_i^{\text{des}}) = (0.3, 0.6, 0.1, 0.5)$, $\forall i \in \mathscr{V}$. $\Delta\sigma_{\text{margin}} = 0.05$. Typical values are derived from [6]. To simulate the variant operation conditions, all loads are scaled with factor ρ_{load}, i.e., $(P_i'^*, Q_i'^*) = \rho_{\text{load}}(P_i^*, Q_i^*)$. All code and data are available on: https://github.com/lingo01/Compositional_Grid_Code.

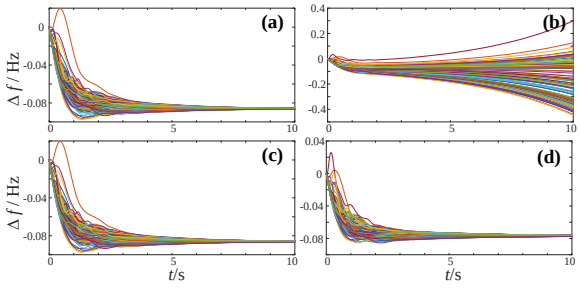

Fig. 3. Transient simulation with satisfying different grid codes. (a) and (b): satisfy only dynamics codes with ρ_{load} =1.0 and 1.2, respectively. (c) and (d): satisfy both stability and dynamics codes with ρ_{load} =1.0 and 1.2. The disturbance is set as +0.05 active power demand of all loads.

If only the dynamics code (6) is satisfied, the transients are depicted in Fig.3(a) and (b) under different ρ_{load}. Conversely, Fig.3(c) and (d) show these with guaranteeing both the stability code (5) and dynamics code (6). Primarily, all tested scenarios adhere to the dynamic code of $\max|\dot{\omega}|_{\text{COI}}^{\text{des}} = 0.1625\text{Hz/s} \leq \sum \Delta P_i / \sum M_i^{\text{des}} = 0.05/0.3 = 0.1667$ Hz/s through the provision of adequate inertia $M_i \geq M_i^{\text{des}}$. Regarding the stability, when ρ_{load} =1.0 ($\sigma_n = -0.448$), Fig.3(a) and (c) indicate that stability is maintained regardless of compliance with stability codes, owing to the relatively stable nature of the grid. However, under weak grids ρ_{load} =1.2 ($\sigma_n = -0.629$), the system only stays stable under the constraint of the stability code as shown in Fig.3(d). Otherwise, it is unstable in Fig.3(b), and certainly, the dynamics code cannot be met. Therefore, adding stability constraints to grid codes is crucial.

VI. Conclusion

This work establishes a unified grid code framework that simultaneously guarantees stability and dynamic performance through distributed control. By reformulating device-grid interactions using passivity theory, we derive a compatible stability grid code. The parametric codes integrate these stability margins with standard dynamic specifications, enabling SOs to coordinate device responses without detailed device models. This approach overcomes prior limitations in stability assurance while supporting plug-and-play integration of IBRs.

References

[1] V. Häberle, L. Huang, X. He, E. Prieto-Araujo, and F. Dörfler, "Dynamic ancillary services: From grid codes to transfer function-based converter control," *Electric Power Systems Research*, vol. 234, p. 110760, 2024.

[2] National Energy System Operator, "THE GRID CODE ISSUE 6 REVISION 33," https://www.neso.energy/industry-information/codes/grid-code-gc/grid-code-documents, 2025.

[3] VDE FNN Hinweis, "Technische Anforderungen an Netzbildende Eigenschaften inklusive der Bereitstellung von Momentanreserve," https://www.vde.com/de/fnn/aktuelles/netzbildende-eigenschaften, 2024.

[4] V. Häberle, A. Tayyebi, X. He, E. Prieto-Araujo, and F. Dörfler, "Grid-forming and spatially distributed control design of dynamic virtual power plants," *IEEE Transactions on Smart Grid*, vol. 15, pp. 1761–1777, 2024.

[5] K. Hassan, *Nonlinear Systems*. Prentice Hall, 1996.

[6] P. Yang, F. Liu, Z. Wang, and C. Shen, "Distributed stability conditions for power systems with heterogeneous nonlinear bus dynamics," *IEEE Transactions on Power Systems*, vol. 35, no. 3, pp. 2313–2324, 2020.

[7] K. Dey and A. M. Kulkarni, "Passivity-based decentralized criteria for small-signal stability of power systems with converter-interfaced generation," *IEEE Transactions on Power Systems*, vol. 38, no. 3, pp. 2820–2833, 2023.

[8] P. Yang, F. Liu, Z. Wang, S. Wu, and H. Mao, "Spectral analysis of network coupling on power system synchronization with varying phases and voltages," in *2020 Chinese Control And Decision Conference (CCDC)*. Hefei, China: IEEE, 2020, pp. 880–885.

[9] X. Peng, C. Fu, Z. Li, P. Yang, Z. Wang, and F. Liu, "Sensitivity conservation and breaking in angle-voltage coupling dynamics," https://doi.org/10.36227/techrxiv.173750053.32180663/v1, 2025.

APPENDIX A
PASSIVITY INDEX OF TYPICAL DEVICES

This section computes the proposed passivity index of several typical devices in inverter-dominant power systems, including the VSG inverters, SGs with secondary frequency regulation, droop-controlled inverters, grid-following (GFL) inverters, and complex control strategies derived from time-domain grid codes.

A. Generator with Secondary Frequency Control Dynamics

The synchronous generator (SG) dynamics with secondary frequency control (SFC) [S1] are written as:

$$G_{\theta,i}=\frac{1}{M_i s^2+(d_i+K_{P,i})s+K_{I,i}},\ G_{V,i}=\frac{1}{\tau_i s+k_i} \tag{8}$$

Substituting this dynamics into (3) and direct computation yields:

$$\tilde{\mathcal{G}}_i(s)=\mathrm{diag}\left[\frac{s}{M_i s^2+(d_i+K_{P,i}-\sigma_i)s+K_{I,i}},\ \frac{s}{\tau_i s+k_i-\sigma_i}\right] \tag{9}$$

Then, similar computations yield that $\tilde{\mathcal{G}}_i$ is passive w.r.t. σ_i if and only if:

$$\boxed{d_i+K_{P,i}>\sigma_i, k_i>\sigma_i} \tag{10}$$

B. P-f and Q-V Droop Dynamics

The P-f/Q-V droop dynamics [S2] are written as:

$$G_{\theta,i}=\frac{D_{p,i}}{\tau_{p,i}s+1},\ G_{v,i}=-\frac{\Delta Q}{\Delta V}=\frac{D_{q,i}}{\tau_{q,i}s+1} \tag{11}$$

First, we consider the phase-angle-related part, the equivalent system of which is written as:

$$\tilde{\mathcal{G}}_i=\frac{D_{p,i}s}{(\tau_{p,i}-\sigma_i D_{p,i})s+1} \tag{12}$$

The first condition of Lemma 1 is satisfied by guaranteeing $\sigma_i<\tau_{p,i}/D_{p,i}$. As for the condition (b), it degenerates to $\Re(\tilde{\mathcal{G}}_i(j\omega))\geq 0, \forall\omega\in\mathbb{R}$ [S3]. For the $P-f$ droop dynamics, direct computation yields:

$$\Re(\tilde{\mathcal{G}}_i(j\omega))=\frac{\omega^2(\tau_{p,i}-\sigma_i D_{p,i})}{1+(\tau_{p,i}-\sigma_i D_{p,i})^2} \tag{13}$$

which is positive if and only if $\sigma_i<\tau_{p,i}/D_{p,i}$. The condition (c) of Lemma 1 does not need to be verified as there are no pure imaginary poles.

Then, we consider the voltage-related part. Noticing the difficulty of frequency-domain analysis, we turn to its time-domain characteristics. In this sense, the voltage dynamic is passive w.r.t. σ_i if there exists a smooth positive semi-definite storage function $S_i(V_i)$ such that:

$$\dot{S}_i(V_i)\leq-(\frac{Q_i}{V_i}-\frac{Q_i^*}{V_i^*})\dot{V}_i-\sigma_i(V_i-V_i^*)\dot{V}_i, \forall(\frac{Q_i}{V_i},V_i) \tag{14}$$

For this case, it is equivalent to the DP defined in [S1]. The equivalence between time-domain and frequency-domain definitions are provided in [S3]. Then, consider the following storage function:

$$S_i(V_i)=\frac{k_i}{D_{q,i}}(\frac{V_i}{V_i^*}-\ln V_i)-\frac{\sigma_i(V_i-V_i^*)^2}{2} \tag{15}$$

where $k_i=V_i^*+D_{q,i}Q_i^*$. Calculating its gradient yields:

$$\nabla S_i=\frac{k_i}{D_{q,i}}(\frac{1}{V_i^*}-\frac{1}{V_i})-\sigma_i(V_i-V_i^*), \nabla^2 S_i=\frac{k_i}{D_{q,i}V_i^2}-\sigma_i \tag{16}$$

Suppose $\sigma_i<k_i/(D_{q,i}V_i^2)$, we have $\nabla S_i(x_i^*)=0$, $\nabla^2 S_i(x_i^*)>0$ and $S_i(V_i)\geq 0$. In addition, its time derivative can be computed as:

$$\dot{S}_i=\frac{k_i}{D_{q,i}}(\frac{1}{V_i^*}-\frac{1}{V_i})\dot{V}_i-\sigma_i(V_i-V_i^*)\dot{V}_i \tag{17}$$

Substituting the voltage droop dynamics into (17) yields:

$$\dot{S}_i=-(\frac{Q_i}{V_i}-\frac{Q_i^*}{V_i^*})\dot{V}_i-\sigma_i(V_i-V_i^*)\dot{V}_i-\frac{\tau_{q,i}}{D_{q,i}V_i}\dot{V}_i^2 \tag{18}$$

which aligns (14). Recalling above derivations only assume $\sigma_i<k_i/(D_{q,i}V_i^2)$, we can conclude that the droop-controlled inverter is passive if:

$$\boxed{\frac{\tau_{p,i}}{D_{p,i}}>\sigma_i, \frac{V_i^*+D_{q,i}Q_i^*}{D_{q,i}(V_i^*)^2}>\sigma_i} \tag{19}$$

C. Dynamics Transformed from Time-Domain Response Requirement

The grid code might be provided by time-domain responses. Here, we use the frequency code as an example. Consider frequency response under normalized active power disturbance as $\Delta\omega_i(t)\leq\alpha_i t$ if $0\leq t\leq t_i^r$ and $\Delta\omega_i(t)\leq\alpha_i t_i^r$ if $t_i^r\leq t\leq t_i^e$. Then, [S4] suggests the control should be designed as:

$$\frac{sG_{\theta,i}}{\alpha_i}=\frac{1}{s}-(t_i^r+\frac{1}{s})\frac{1-\frac{t_i^r}{2}s}{1+\frac{t_i^r}{2}s}+t_i^r\frac{1-\frac{t_i^r}{2}s}{1+\frac{t_i^r}{2}s}-t_i^r\frac{1-\frac{t_i^e}{2}s}{1+\frac{t_i^e}{2}s} \tag{20}$$

Substitute it into (3) and the denominator of $\tilde{\mathcal{G}}_i$ is:

$$\begin{aligned}DEN=&t_i^e t_i^r(1-\alpha_i t_i^r\sigma_i)(s^2+1)\\&+[t_i^e+t_i^r+(t_i^r)^2\alpha_i\sigma_i-3t^e t^r\alpha_i\sigma_i]s\end{aligned} \tag{21}$$

Therefore, the dynamics are passive if and only if:

$$\sigma_i<\frac{1}{\alpha_i t_i^r}, \sigma_i<\frac{t_i^e+t_i^r}{3t_i^e t_i^r\alpha_i-(t_i^r)^2\alpha_i} \tag{22}$$

Suppose $t_i^e\to\infty$, i.e., the device is required to provide steady power injection. Then, the above condition degenerates to:

$$\boxed{\frac{1}{3\alpha_i t_i^r}>\sigma_i} \tag{23}$$

Remark 1 (*Trade-off between grid codes*)**.** It is worth recognizing that stability code might not be met with improper dynamics code without careful design. Specific to this case, once the stability code σ_i^{des} decided, the dynamic code t_i^r, t_i^e, α_i should be carefully designed to satisfy $1/(3\alpha_i t_i^r)\geq\sigma_i^{\mathrm{des}}$.

D. Grid-Following Dynamics with Phase-Lock Loop

For GFL devices $i \in \mathscr{V}$ with f-P and V-Q droop controls, a classical model [S2], [S5], [S6] can be written as:

$$\begin{aligned} G_{\theta,i} &= \left[\frac{d_{p,i}}{\tau_{p,i}s+1}\frac{s(K_{P,i}V_i^*s+K_{I,i}V^*)}{s^2+K_{P,i}V_i^*s+K_{I,i}V^*}\right]^{-1} \\ G_{V,i} &= \left[\frac{d_{q,i}}{\tau_{q,i}s+1}\right]^{-1} \end{aligned} \tag{24}$$

where $K_{P,i}$ and $K_{I,i}$ are PI parameters of the phase-lock loop (PLL), and d_p and d_q are $f-P$ and $V-Q$ droop gains, respectively.

It is noted that the relative degree of both $G_{\theta,i}$ and $G_{V,i}$ is negative since the GFL devices have distinct input-output causality compared to the GFM counterparts. Here we consider their causal approximation with artificial inertia ε. Specifically, the dynamics can be approximated by:

$$\begin{aligned} G_{\theta,i} &\approx \frac{G_{\theta,i}}{(\varepsilon s+1)^2} = \frac{(\tau_{p,i}s+1)/d_{p,i}}{(\varepsilon s+1)^2}\frac{s^2+K_{P,i}V^*s+K_{I,i}V_i^*}{s(K_{P,i}V_i^*s+K_{I,i}V_i^*)} \\ G_{V,i} &\approx \frac{G_{V,i}}{(\varepsilon s+1)^2} = \frac{(\tau_{q,i}s+1)/d_{q,i}}{(\varepsilon s+1)^2} \end{aligned} \tag{25}$$

It is no wonder that the expression can precisely approximate the original one in the concerned bandwidth if setting $1/\varepsilon \gg 1/\tau_p, 1/\tau_q$. Typically, $\varepsilon = 10^{-4}$s can be chosen, since the phasor model inherently can only describe the electromechanical transience under 10^2 Hz. The detailed investigation of this approximation can be found in [S7].

Then, conduct a similar procedure to compute the $\tilde{\mathcal{G}}_i$ and identify its passivity. The denominators of $\tilde{\mathcal{G}}_i$ are respectively

$$\begin{aligned} DEN_p = &(\varepsilon^2 K_{P,i} - \frac{\sigma_i}{d_p}\tau_{p,i})s^3 \\ &+ [2\varepsilon K_{P,i} + \varepsilon^2 - \frac{\sigma_i}{d_p}(K_{P,i}\tau_{p,i}+1)]s^2 \\ &+ [2\varepsilon K_{I,i} + K_{P,i} - \frac{\sigma_i}{d_{p,i}}(K_{P,i}+K_{I,i}\tau_{p,i})]s \\ &+ K_{I,i}(1-\frac{\sigma_i}{d_{p,i}}) \\ DEN_q = &\varepsilon^2 s^2 + (2\varepsilon - \frac{\sigma_i}{d_{q,i}}\tau_{q,i})s + (1-\frac{\sigma_i}{d_{q,i}}) \end{aligned} \tag{26}$$

The passivity condition can be obtained similarly. As $\varepsilon \to 0$, the corresponding $\tilde{\mathcal{G}}_i$ can be passive if and only if:

$$\boxed{\sigma_i \to 0} \tag{27}$$

In other words, the GFL devices with $\sigma_i \to 0$ generally do not help the transient stability of power systems compared to GFM devices with positive $\sigma_i > 0$, which also aligns with the practice observation.

An alternative formulation to consider GFL dynamics is the dual passivity structure developed in [S8]. This approach is technically more complex but can consider more precise GFL dynamics such as PLL bandwidth and $f-P/V-Q$ droop coefficient. This can be achieved by simply following the methodology of [S8].

APPENDIX B
COMPARISON WITH EXISTING WORKS

This section describes the advancements of the proposed method compared to existing approaches in two aspects: further extension of passivity theory and stronger application potential in power system stability assessment and grid code synthesis.

A. Extended Passivity Theory

The proposed method extends the analytical framework of passivity, thereby broadening its theoretical applicability. The classical passivity, existing extensions in the literature, and the proposed generalization framework are illustrated in Fig.4 with detailed explanations provided below:

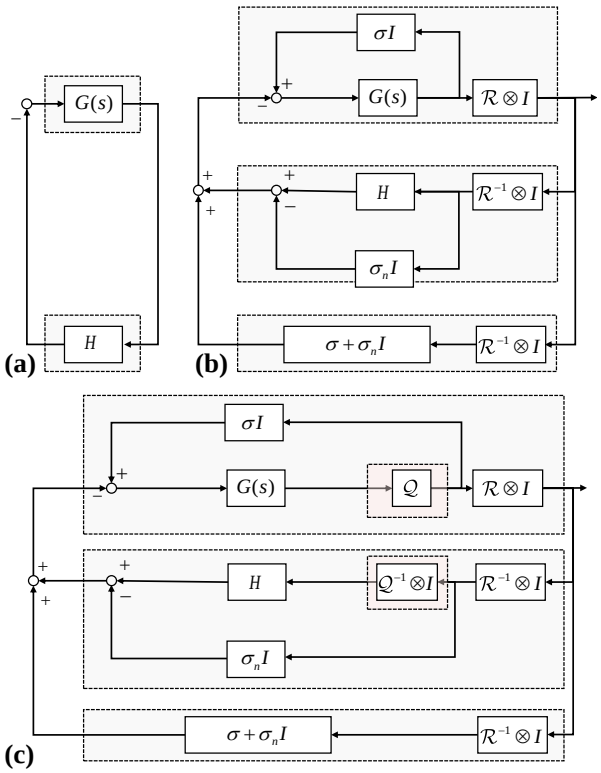

Fig. 4. Extension of passivity theory. (a): classical passivity. (b): the existing works only involve the input/output mapping changes to extend passivity theory. (c): the proposed work involves both input/output mapping and topology changes.

1) Classical Passivity: As shown in Fig.4(a), classical passivity requires that both transfer functions G and H are passive individually [S3], so that the feedback-interconnected system is also passive and hence stable. However, this requirement is often too strict for practical systems.

2) Input Feedforward Passivity (IFP) and Output Feedback Passivity (OFP): The topology is shown in Fig.4(b), where $\mathcal{R} = \text{diag}(1,1)$. To relax the requirements of classical passivity, IFP and OFP are usually employed [S3]. Note that it reduces to classical passivity when $\sigma = \sigma_n = 0$.

3) IFP and OFP with Input/Output Mapping Operators: The topology remains as in Fig.4(b), but here $\mathcal{R}$ may be an operator, often chosen as a linear operator related to s,

referred to as an input/output mapping operator. For example, the DP defined in [S1], [S6] uses $\mathcal{R} = \text{diag}(s, s)$, while [S9] adopts a form $\mathcal{R} = \text{diag}(s/(1+\varepsilon s), s/(1+\varepsilon s))$. The purpose of introducing such differential-like structures is to make practical power system devices more easily satisfy passivity under this input/output mapping.

4) Proposed Passivity: The topology is shown in Fig.4(c), where $\mathcal{R} = \text{diag}(s, 1)$ and $\mathcal{Q} = \text{diag}(1, s)$. Although the modification from Fig.4(b) appears minor, it fundamentally changes the topological structure of the passivity definition. Taking OFP/ODP as an example (similar for input feedforward IFP and IDP), in Fig.4(b), the modification $\mathcal{R}$ for achieving passivity is applied outside the feedback loop, whereas Fig.4(c) introduces an additional degree of freedom inside the feedback loop via $\mathcal{Q}$, making it easier for devices to satisfy passivity.

In summary, the proposed passivity analysis framework in Fig.4(c) is a further extension of existing frameworks. While existing methods focus on designing the input/output mapping operator within the same topology Fig.4(b), we directly extend the framework at the topological level. By choosing different mapping operators $\mathcal{R}$ and $\mathcal{Q}$ and values of the index σ, the proposed framework can reduce to existing methods. Therefore, the proposed framework further broadens the applicability of passivity theory.

B. Application to Grid Code

When applied to power system stability analysis and grid code design, the proposed method also demonstrates advantages over existing indices, as shown below:

1) Compatibility with Devices That Can Be Passivated Under Classical IFP/OFP and IDP/ODP Frameworks: As shown in Appendix A, SGs with SFC and inverters with P-f/Q-V droop control can still be passivated under the proposed framework.

2) Enabling Passivation of Previously Non-Passivable Devices: Under the classical IFP/OFP framework with $\mathcal{R} = \mathcal{Q} = (1, 1)$, SGS and VSGs struggle to be passive due to low frequency non-passivity [S9], [S10]. Thus, although practice shows that pure-SG/VSG systems can be stable, it cannot be proven under the classical passivity framework, indicating their conservation. The DP theory [S1] offers some improvement, allowing devices with SFC dynamics (8) to achieve a positive passivity index and enabling subsequent distributed stability analysis. However, for classical SG/VSG dynamics (4), it still cannot provide a positive passivity index, making it difficult to meet the condition $\sigma_i' > -\sigma_n > 0$, and hence unable to support distributed stability verification or grid code synthesis. In contrast, the proposed method can passivate and assess stability for such devices, as shown in the main text. Moreover, devices that are difficult to analyze using existing methods, such as (20), can also be passivated using the proposed approach.

Remark 2. It is important to distinguish between the *physical modeling frequency bands* and *passivity-based stability assessment frequency bands*. The former describes the concerned and modeled timescale of power system dynamics, while the latter is for stability assessment in the sense of control theory. Both our approach and [S9], [S10] utilize phasor-based models, describing system dynamics at electromechanical timescales, such as synchronization dynamics and voltage control loops.

However, to guarantee stability of feedback interconnected systems through passivity-based methods, the passivity conditions must hold across all frequencies, i.e., $G(j\omega)$ must satisfy the conditions of Lemma 1 for all ω. In [S9], [S10], the passivity under the classical definition cannot be assured for SG/VSG models in high-frequency bands using polar coordinates, so stability cannot be guaranteed. Consequently, they apply a timescale separation assumption and adopt polar and rectangular coordinates at low and high frequencies, respectively, to partially establish passivity.

By contrast, this work fundamentally reformulates the output mapping and system topology of passivity definition, allowing the SG/VSG models to be passive (in an extended sense) over the entire frequency bands without a timescale separation assumption or coordinate switching. This innovation enables distributed passivity criteria, and thus stability, to be established directly for grid code generation.

3) Enabling Stability Assessment for Previously Unverifiable Systems: The proposed method is fully compatible with the stability conditions of DP theory [S1]. According to the following Lemma 2, the network can retain the same index $\sigma_n = \lambda_{\min}(C - D^T A^\dagger D) \leq 0$ for both the original DP and the proposed theory. Therefore, stability can be verified in a distributed manner if the device satisfies either the ODP index $\sigma_i' > -\sigma_n$ or the proposed one $\sigma_i > -\sigma_n$.

Lemma 2. For a power system $\mathscr{G}$, define its network passivity derived from the original DP theory by $\sigma_n' = \lambda_{\min}(H)$ [S1] and the proposed one by σ_n. Then, under the conditions of Theorem 1, it holds $\sigma_n \leq \sigma_n'$.

Proof. The following identity holds due to the generalized Schur's formula [S11], where the network dynamics $H = [A, D; D^T, C]$ and $\Gamma = C - D^T A^\dagger D$.

$$\begin{bmatrix} I & \\ -(A^\dagger D)^T & I \end{bmatrix} \begin{bmatrix} A & D \\ D^T & C \end{bmatrix} \begin{bmatrix} I & -(A^\dagger D)^T \\ & I \end{bmatrix} = \begin{bmatrix} A & \\ & \Gamma \end{bmatrix} \tag{28}$$

Then, minus $\text{diag}(0, \sigma_n I)$ on both sides of the equation. The right-hand side is positive definite since $A \succ 0$ and $C - D^T A^\dagger D - \sigma_n I \succ \lambda_{\min}(C - D^T A^\dagger D) - \sigma_n I \succ 0$.

The inertia of the matrix $H - \text{diag}(0, \sigma_n I)$ and $\text{diag}(A, C - D^T A^\dagger D - \sigma_n I)$ are identical due to the invariant nature of congruent transformations, which suggests the left-hand side $H - \text{diag}(0, \sigma_n I) \succ 0$ if and only if the right-hand side is positive definite. Then, as $\sigma_n \leq 0$, we can obtain:

$$\begin{bmatrix} A - \sigma_n I & D \\ D^T & C - \sigma_n I \end{bmatrix} \succeq \begin{bmatrix} A & D \\ D^T & C - \sigma_n I \end{bmatrix} \succ 0 \tag{29}$$

In other words, the matrix $H - \sigma_n I$ is passive w.r.t. σ_n. Meanwhile, indicated by its definition, σ_n' is the maximum value s.t. $H - \sigma_n' I$ is passive, and thus, we can conclude $\sigma_n \leq \sigma_n'$. □

The proof implies that the system is passive w.r.t. σ_n' if it is passive w.r.t. σ_n. Therefore, the network can retain the same

index $\sigma_n = \lambda_{\min}(C - D^T A^\dagger D) \leq 0$ for both the original DP and the proposed theory

For example, for SG with SFC dynamics, DP theory requires $\sigma_i' = \min(K_{I,i}, k_i) > -\sigma_n$ for stability, while the proposed index requires $\sigma_i = \min(d_i + K_{P,i}, k_i) > -\sigma_n$. Due to the consistency of the network index σ_n, stability can now be ensured under the less conservative condition:

$$\min(d_i + K_{P,i}, K_{I,i}, k_i) > -\sigma_n \tag{30}$$

4) Ability to Account for Key Dynamics: A well-known limitation of energy-function-based stability analysis methods is their difficulty in accounting for the effect of frequency-damping terms d. In the construction of the storage or energy function, d often appears as a dissipation term that ensures negative definiteness of the derivative, i.e., $\dot{E} \leq -d\omega^2 +$ other negative terms. Consequently, frequency dissipation terms often do not appear in stability indices. Even with various extensions [S12], [S13], its distributed application in inverter-integrated systems remains restricted. While this does not significantly impact stability conclusions, it noticeably affects system dynamic performance (especially phase-angle and frequency dynamics) and must be considered in grid code specifications. The proposed method successfully addresses this requirement compared to the existing works [S1].

REFERENCES

[1] P. Yang, F. Liu, Z. Wang, and C. Shen, "Distributed stability conditions for power systems with heterogeneous nonlinear bus dynamics," *IEEE Transactions on Power Systems*, vol. 35, no. 3, pp. 2313–2324, 2020.

[2] X. Peng, C. Fu, Z. Li, P. Yang, Z. Wang, and F. Liu, "Sensitivity conservation and breaking in angle-voltage coupling dynamics," https://doi.org/10.36227/techrxiv.173750053.32180663/v1, 2025.

[3] K. Hassan, *Nonlinear Systems*. Prentice Hall, 1996.

[4] V. Häberle, L. Huang, X. He, E. Prieto-Araujo, and F. Dörfler, "Dynamic ancillary services: From grid codes to transfer function-based converter control," *Electric Power Systems Research*, vol. 234, p. 110760, 2024.

[5] L. Huang, H. Xin, W. Dong, and F. Dörfler, "Impacts of grid structure on PLL-synchronization stability of converter-integrated power systems," *IFAC-PapersOnLine*, vol. 55, no. 13, pp. 264–269, 2022.

[6] P. Yang, "Augmented synchronization based stability theory and its distributed analytics of power systems," Ph.D. dissertation, Tsinghua Univeristy, Beijing, 2022.

[7] X. Peng, X. Ru, J. Zhang, T. Jiang, X. Chen, and F. Liu, "On the damping redistribution mechanism of angle-voltage coupling dynamics in power systems with hybrid gfm-gfl devices," *accepted by IEEE PES ISGT Europe Conference 2025*, 2025.

[8] Z. Li, B. Zeng, X. Peng, M. Wang, X. Ru, Y. Wang, and F. Liu, "Distributed stability analysis for power systems with grid-following and grid-forming devices," in *4th Energy Conversion and Economics Annual Forum (ECE Forum 2024)*, vol. 2024, 2025, pp. 1463–1470.

[9] K. Dey and A. M. Kulkarni, "Passivity-based decentralized criteria for small-signal stability of power systems with converter-interfaced generation," *IEEE Transactions on Power Systems*, vol. 38, no. 3, pp. 2820–2833, 2023.

[10] ——, "Analysis of the Passivity Characteristics of Synchronous Generators and Converter-Interfaced Systems for Grid Interaction Studies," *International Journal of Electrical Power & Energy Systems*, vol. 129, p. 106818, 2021.

[11] P. Yang, F. Liu, Z. Wang, S. Wu, and H. Mao, "Spectral analysis of network coupling on power system synchronization with varying phases and voltages," in *2020 Chinese Control And Decision Conference (CCDC)*. Hefei, China: IEEE, 2020, pp. 880–885.

[12] Y.-H. Moon, B.-K. Choi, and T.-H. Roh, "Estimating the domain of attraction for power systems via a group of damping-reflected energy functions," *Automatica*, vol. 36, no. 3, pp. 419–425, 2000.

[13] W. Ding, C. He, H. Geng, and Y. Liu, "A Novel Lyapunov Function for Transient Synchronization Stability Analysis of Grid-Following Converters," *IEEE Transactions on Power Systems*, 2025.